

Simulating Annealing Speed and Current Controllers Optimization for PMBLDC Motor Drive Systems

MAAD SHATNAWI^{1*} and EHAB BAYOUMI²

¹Department of Electrical Engineering Technology, Higher Colleges of Technology, Abu Dhabi, UAE

²Department of Power Electronics and Energy conversion, Electronics Research Institute, Cairo, EGYPT

*Corresponding Author's Email: maad.shatnawi@hct.ac.ae

Abstract: - Brushless Direct Current (BLDC) motors have several advantages including high efficiency and high speed ranges and accordingly are commonly used in a broad range of industrial applications. To accommodate the high performance requirement of the modern industry, optimization of the proportional-integral (PI) and proportional-integral-derivative (PID) controller parameters are highly explored and several tuning methods have been suggested. This work demonstrates a robust permanent magnet brushless dc motor (PMBLDCM) controller design method where a simulated annealing algorithm is employed to tune the parameters of a PI current controller and a PID speed controller of the motor. Three response performance parameters including overshoot, rise time, and settling time are simultaneously optimized during the tuning process. To enhance the overall performance of the system under wide loading conditions, a set of operating points is considered within the objective function. The technique is compared to both Particle Swarm Optimization and Ziegler-Nichols tuning methods and results show the superiority of the proposed approach.

Key-Words: - Simulated annealing, multiobjective optimization, PID controller, brushless dc motor, PMBLDCM.

1 Introduction

Brushless Direct Current (BLDC) motors are characterized by their high power-savings, long operating life, noiseless operation, high speed ranges, high power-to-weight ratio and high efficiency, and therefore, they are commonly used in a wide range of applications including aerospace, automotive, medical, automation and instrumentation equipment [1-9]. The proportional-integral (PI) and proportional-integral-derivative (PID) controllers are intensely studied in various research papers. These controllers start their attractiveness since the classic Ziegler-Nichols method [10] was presented.

There are a variety of tuning approaches proposed to adapt the exceptional requirement of contemporary industry optimization to the PID parameters such as, gain and phase margin method [11], the internal model control (IMC) based PID tuning method [12, 13] and decay ratio method [14]. Moreover, with the recognition of the interior point technique many PID design approaches using Linear Matrix Inequality (LMI) were recommended for the continuous-time systems [15, 16]. Furthermore, PID parameters fine-tuning with state –feedback linear quadratic regulator (LQR) is given in [17].

Evolutionary computations with stochastic search techniques are more capable approach to solve the controller parameters estimation problem. The evolutionary computation for controller parameters

identification is applied on BLDC motor drive system. Genetic algorithm (GA) is used to identify the controller parameters of the motor [18]. An evolutionary algorithm based on Particle Swarm Optimization (PSO) with weighting factors has also been introduced and tested on induction motor [19]. In [20] a PSO algorithm with constriction factor is proposed to recognize the controller parameters of the BLDC motor where the controllers' parameters are tuned to attain a deed beat maximum over index only. It should be noted that even the most successful nature-inspired optimization techniques, such as GA and PSO are also sensitive to the increase of the problem complexity and dimensionality, due to their stochastic nature [21]. In last decade, more attention is given to bacterial foraging optimization (BFO) which has a rich source of potential engineering applications and computation. A few models have been obtained to represent bacterial foraging behaviors and applied it for solving practical problems [22]. Among them, BFO is a population-based numerical optimization algorithm. It solved these engineering problems successfully. But, in complex optimization problems the original BFO algorithm reveals a slow convergence behavior and its performance also heavily decreases with the growth of the search space dimensionality [23].

This paper introduces a robust design approach for PMBLDCM drive current and speed controllers where a Simulated Annealing algorithm is employed to tune

the parameters of PID/PI controllers. The maximum overshoot, rise time and settling time are all simultaneously minimized within the tuning process. The proposed algorithm is evaluated and compared with both the Particle Swarm optimization and Ziegler-Nichols tuning technique.

This paper is organized as follows. Section 2 introduces the overall block diagram of PMBLDCM drive system. Section 3 presents the PI/PID controllers optimization with minimal overshoot, rise time, and settling using SI technique. The results of the proposed approach are presented in Section 4. Section 5 provides some conclusion remarks on the proposed approach for controlling PMBLDCM drive system.

2 PMBLDCM DRIVE SYSTEM

The mathematical model of PMBLDCM drive is given in [20, 24]. The overall block diagram of the drive system is given in Fig. 1 where

- R_s : stator resistance per phase.
- L_s : stator inductance per phase.
- e : stator voltage per phase.
- ω_m : rotor speed.
- v_s : stator voltage.
- i_s : stator current.
- T_e : electromagnetic torque.
- T_L : load torque.
- K_T : load torque constant.
- K_b : flux constant (volt/rad/sec).
- B : motor friction.
- J : moment of inertia of PMBLDCM.

3 Simulated Annealing

Simulated Annealing (SA) is an effective optimization technique introduced by Kirkpatrick et al. [25] as a computational analogous to the annealing process which is the heating and controlled cooling of a metal to increase the size of its crystals and reduce their defects. The function to be optimized in SA is called the energy, $E(x)$, of the state x , and during that, a parameter T , the computational temperature, is lowered throughout the process. SA is an iterative trajectory descent algorithm that keeps a single candidate solution at any time [26, 27].

The major advantage of SA is its ability to avoid being trapped in local optima. This is because the algorithm applies a random search which does not only accept changes that improve the objective function, but also some changes that temporarily worsen it [28, 29]. Geman and Geman [30] presented evidence that simulated annealing guarantees to converge to the global optimum if the cooling schedule is adequately slow. On the other hand, [31, 32] reported through experience that SA shows a very effective optimization performance even with relatively rapid cooling schedules [33]. SA is commonly found in industry and provides good results [26, 27]. SA have been examined and showed a well performance in a variety of single-objective and multiobjective optimization applications as reported by several researchers. Some of these applications are wireless telecommunications networks [27, 32, 34], nurse scheduling problems [35], high-dimensional and complex nanophotonic engineering problems [36], pattern detection in seismograms [37], gene network model optimization [38], and multiple biological sequence alignment [39- 41].

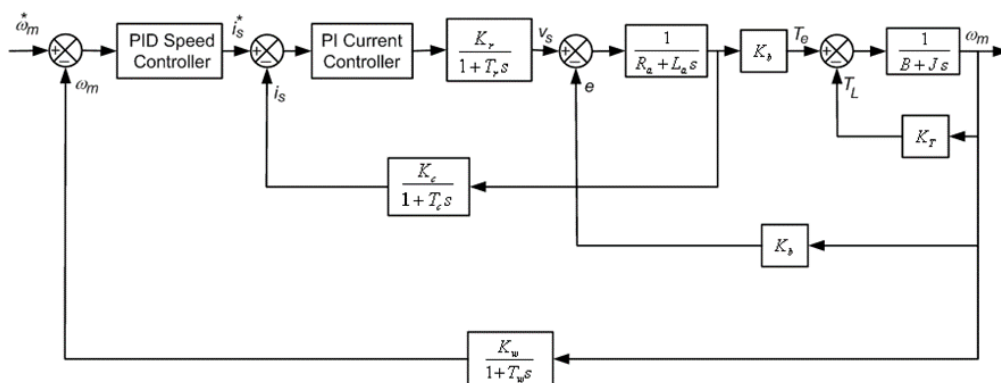


Fig. 1 Overall block diagram of proposed control for PMBLDCM drives system.

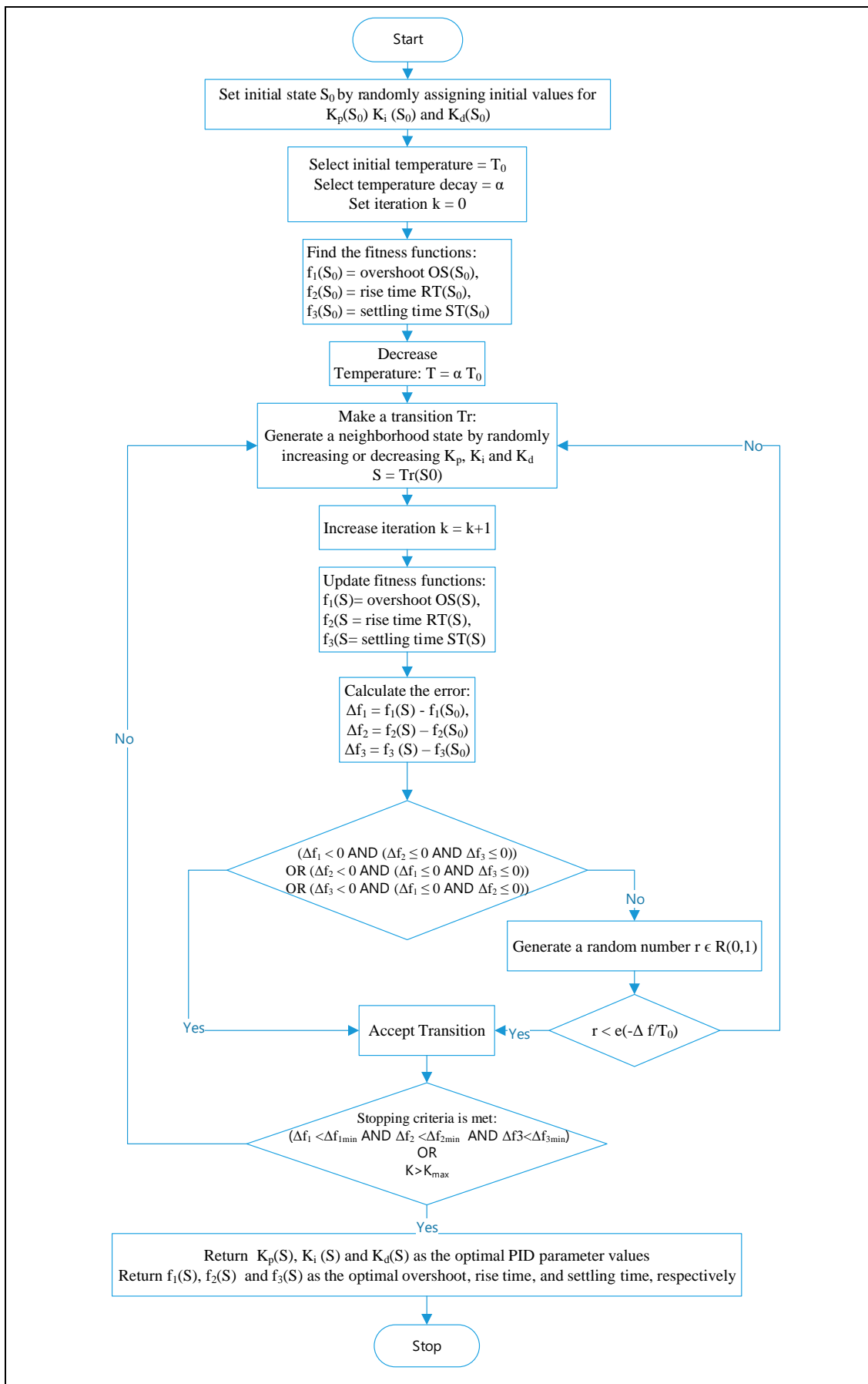


Fig. 2 Simulated Annealing for PI/PID Controller Optimization.

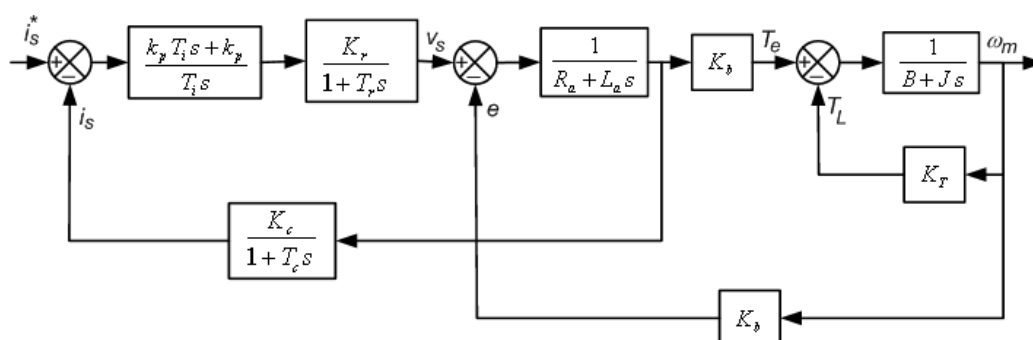


Fig. 3 The current control loop of PMBLDCM drive system.

We employed the Simulated Annealing (SA) technique to optimize PI and PID controller parameters. This is a multiobjective optimization problem where three parameters of controller step response are simultaneously minimized. During the optimization process, SA will accept a transition from state S_1 to another state S_2 if S_2 dominates S_1 , that is if S_2 is not worse for all objectives than S_1 and entirely better for at least one objective. In other words, SA will accept a transition that leads to a decrease in all objectives (overshoot, rise time and settling time) or a decrease in one of the objectives if other objectives are not changed. SA will also accept a transition from state S_1 to S_2 if S_2 does not dominate S_1 with a probability of $e^{-\Delta f/T}$, where $\Delta f = f(S_2) - f(S_1)$, and T is the temperature parameter which is being reduced over time during the optimization process in order to decrease the possibility of accepting such transitions. The proposed optimization algorithm is illustrated in Fig. 2.

4.1 Current Control of PMBLDCM

The block diagram of the current control loop of PMBLDCM drive system is given in Fig. 3. The PM BLDCM contains an inner loop due to the back emf. The current loop will cross this back emf loop, creating a complexity in the development of the model. The interactions of these loops can be decoupled by suitable redrawing the block diagram. The open loop transfer function of the current control loop is:

$$G_{current_openloop} = \frac{k_p K_r K_c (1 + T_i s)}{T_i s (1 + T_r s) (R_a + L_a s) (1 + T_c s)} \quad (1)$$

where,

- K_r : Gain of the inverter.
- T_r : Time constant of the inverter.
- K_c : Gain of the current transducer.
- T_c : Time constant of the current transducer.

4.2 Current Controller Optimization

The PI current controller transfer function is

$$G_c(s) = \frac{k_p T_i s + k_p}{T_i s} \quad (2)$$

Our objective is to find the optimal PI parameters that stabilizes the system with minimal overshoot, rise time, and settling time response over the operating range. The parameters k_p and T_i of the PI controller are randomly initialized and then SA is applied to optimize k_p and T_i to achieve minimal overshoot, rise time, and settling time. Fig. 4 shows the values of these fitness functions during SA iterations.

The optimal k_p achieved by SA is 0.932 and the optimal T_i is 0.001765. The resulting PI controller is

$$G_{PI}(s) = \frac{0.001645 s + 0.932}{0.001765 s} \quad (3)$$

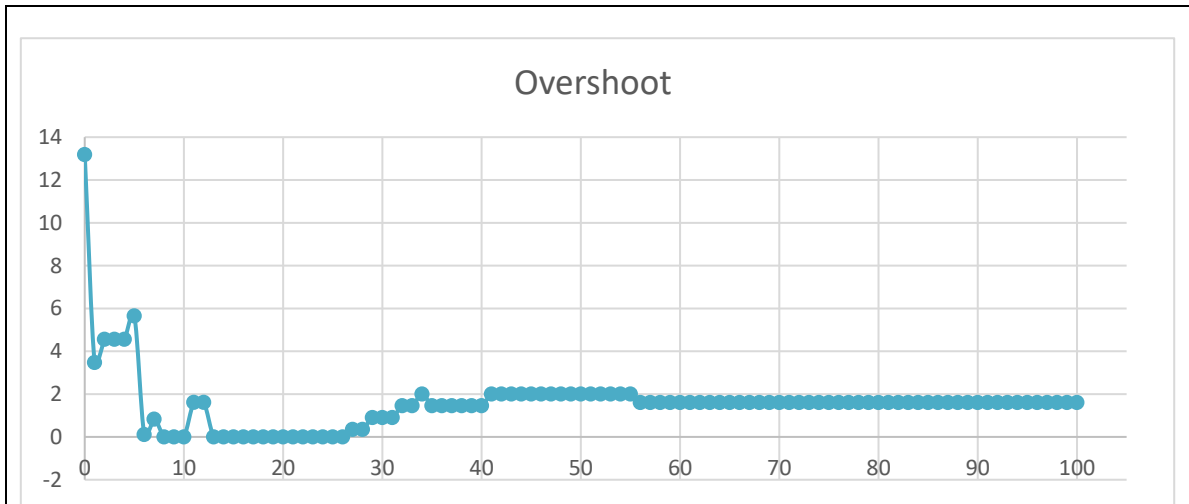
4.3 Speed Control of PMBLDCM

The block diagram of the speed control loop of PMBLDCM drive system is given in Fig. 5. The PMBLDCM contains three inner loops creating a complexity in the development of the model. Mason's rule is applied to reduce the block diagram as shown in Fig. 6.

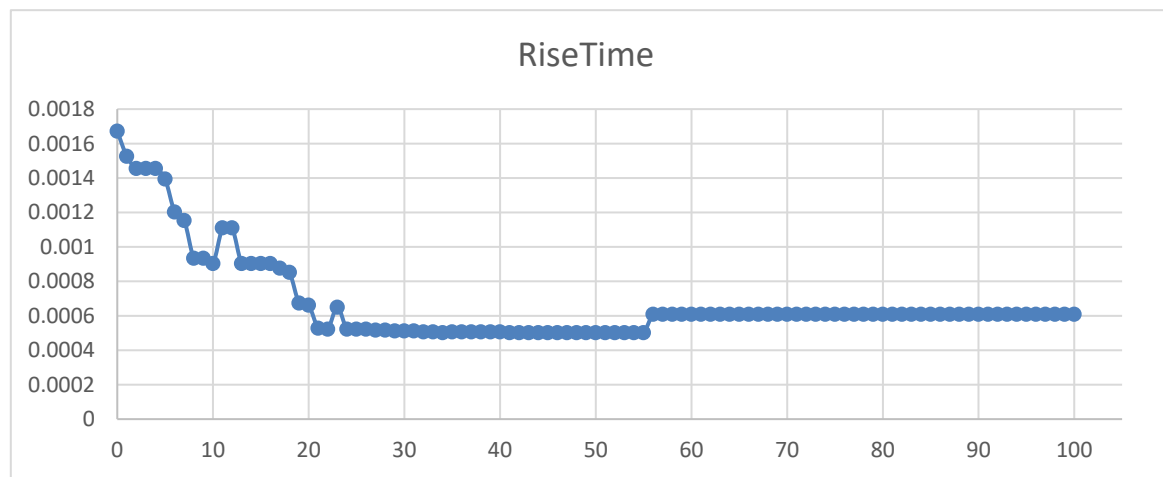
$$G_{sys} = \frac{\omega_m(s)}{I_s^*(s)} = \frac{P}{1 + (L_1 + L_2 + L_3) + L_1 L_2} \quad (4)$$

where the forward path, loop gains are respectively given as

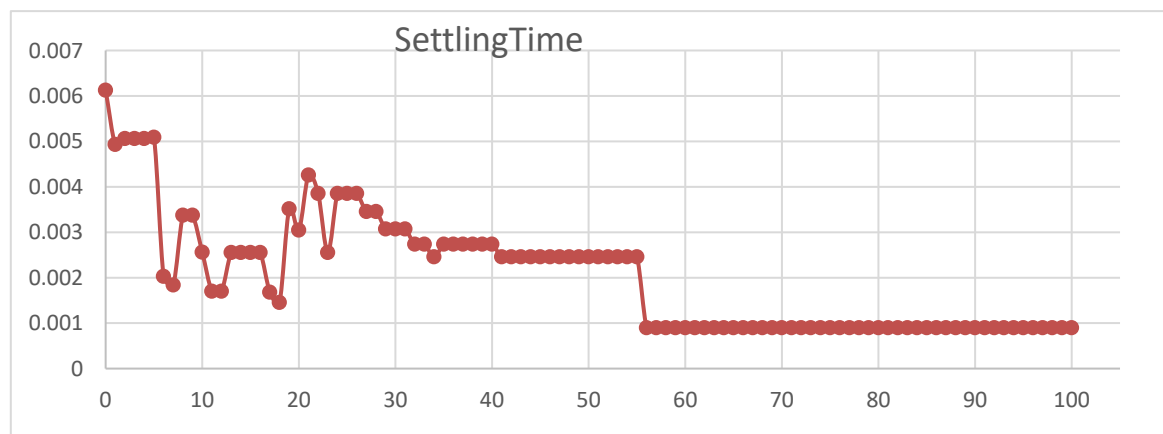
$$P = \frac{k_p K_r K_b (1 + T_i s)}{T_i s (1 + T_r s) (R_a + L_a s) (B + J s)} \quad (5)$$



(A) Maximum overshoot vs. iterations.



(B) Rise time vs. iterations.



(C) Settling time vs. iterations.

Fig. 4 Maximum overshoot, rise time and settling time for the PI current controller during the optimization process.

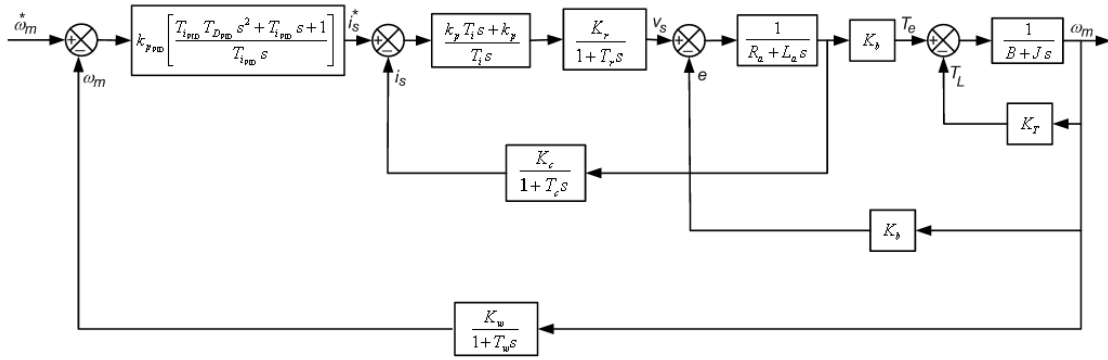


Fig. 5 Block diagram of the speed control loop for PMBLDCM.

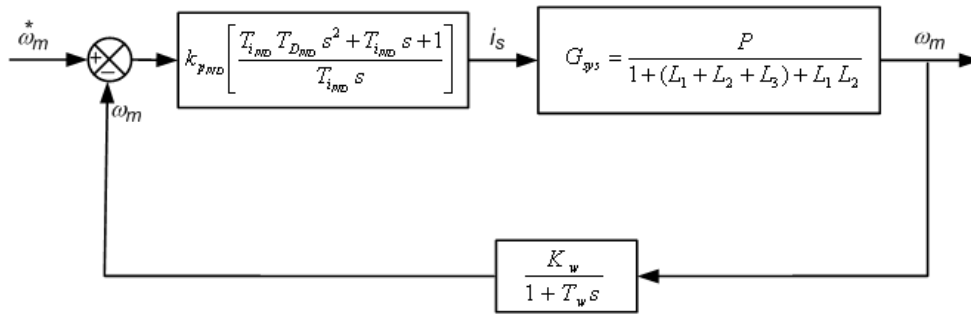


Fig. 6 Reduced block diagram of the speed control loop for PMBLDCM.

$$L_1 = -\frac{k_p K_r K_c (1 + T_i s)}{T_i s (1 + T_r s) (R_a + L_a s) (1 + T_c s)} \quad (6)$$

$$L_2 = -\frac{K_T}{(B + J s)} \quad (7)$$

$$L_3 = -\frac{K_b^2}{(R_a + L_a s) (B + J s)} \quad (8)$$

The open loop transfer function of the speed control loop is:

$$G_{speed_openloop} = \frac{k_{pPID} P K_w (T_{iPID} T_{dPID} s^2 + T_{iPID} s + 1)}{T_{iPID} s (1 + (L_1 + L_2 + L_3) + L_1 L_2) (1 + T_w s)} \quad (9)$$

where,

K_w : Gain of speed transducer.

T_w : Time constant of speed transducer.

$k_{pPID}, T_{iPID}, T_{dPID}$: Parameters of the PID controller.

4.4 Speed Controller Optimization

The PID speed controller transfer function is

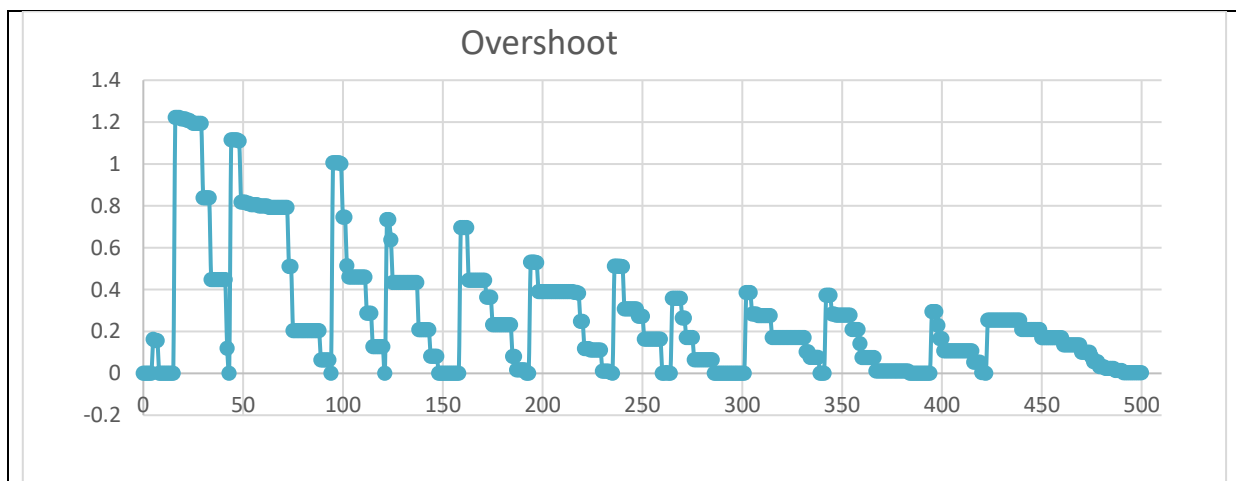
$$G_s(s) = k_p \frac{T_i T_d s^2 + T_i s + 1}{T_i s} \quad (10)$$

The parameters k_{pPID}, T_{iPID} and T_{dPID} of the PID controller are randomly initialized. SA is applied to optimize k_{pPID}, T_{iPID} and T_{dPID} to achieve minimal overshoot, rise time, and settling time. Figure 6 shows the values of the fitness functions during the optimization iterations.

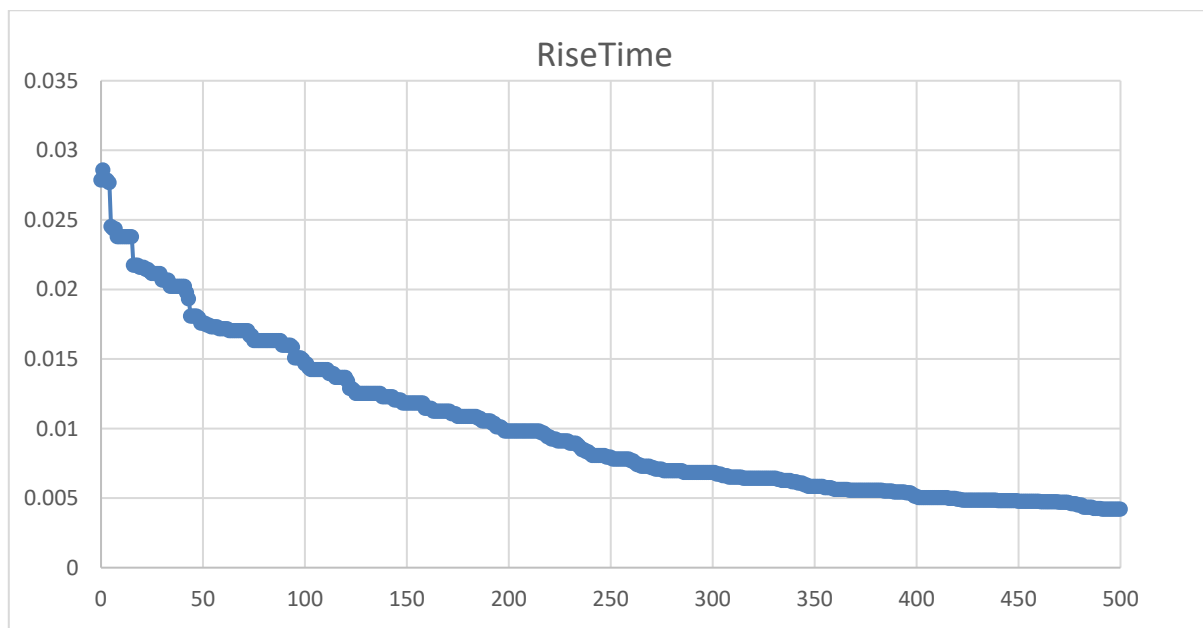
The parameters k_{pPID}, T_{iPID} and T_{dPID} of the PID controller are randomly initialized. SA is applied to optimize k_{pPID}, T_{iPID} and T_{dPID} to achieve minimal overshoot, rise time, and settling time. Fig. 7 shows the values of the fitness functions during the optimization iterations.

The optimal k_p achieved by SA is 14.6265, the optimal T_i is 0.0448, and the optimal T_d is 0.0000102553. The resulting PID controller is

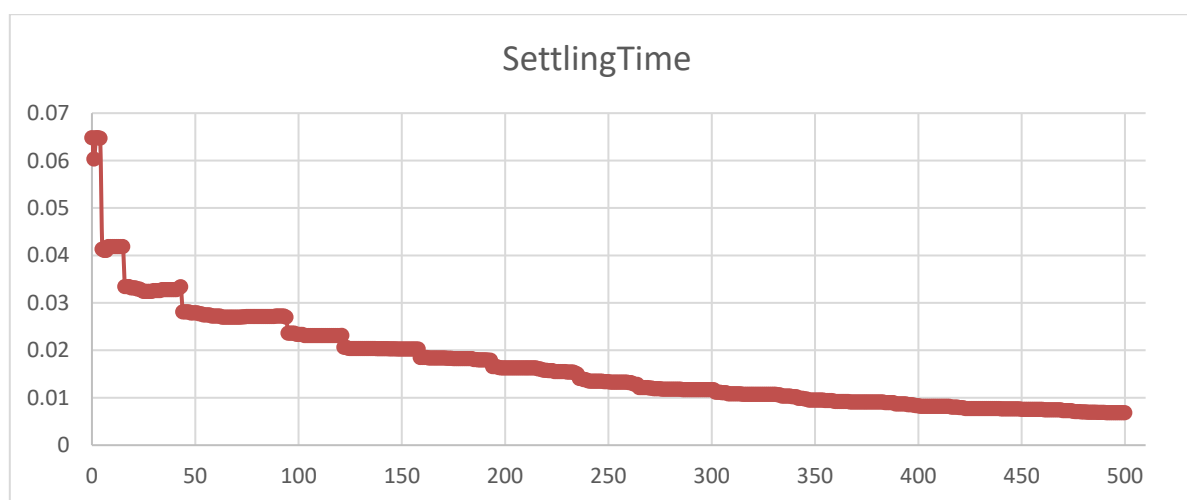
$$G_{PID}(s) = 14.6265 \frac{(4.596 \times 10^{-7} s^2 + 0.0448 s + 1)}{0.0448 s} \quad (11)$$



(A) Maximum overshoot vs. iterations.



(B) Rise time vs. iterations.



(C) Settling time vs. iterations.

Fig. 7 Maximum overshoot, rise time and settling time for the PID speed controller during the optimization process.

6 Results

The PI current controller and PID speed controllers are designed with minimal overshoot, rise time and settling time using SA optimization technique. In Fig. 8, the PI controller designed is tested at three loading conditions; heavy, nominal, and light. These are represented respectively as 150%, 100% and 50% of armature resistance R_a . It is shown that, in the worst case, the maximum overshoot is 7.8% (at $R_a=50\%$ of the rated value).

To evaluate the SA PI controller, we compare it with both PSO and ZN controllers. The PI current controller of the PMBLDCM drive system using Ziegler-Nichols PI tuning technique was designed on the rated armature resistance (R_a) and then tested on 50% and 150% of R_a . The transfer function of PI speed controller designed by Ziegler-Nichols [11] is given by

$$G_{PI_ZN} = \frac{0.003623s + 6.67}{5.44 \times 10^{-4} s} \quad (12)$$

where $K_p = 6.67$, $T_i = 5.44 \times 10^{-4}$, $K_i = 12261$.

The transfer function of the PSO PI current controller designed by [20] is given by

$$G_{PI_PSO}(s) = \frac{0.01063s + 1.9816}{0.0054s} \quad (13)$$

where $K_p = 1.9816$, $T_i = 0.0054$, $K_i = 24.04 \times 10^6$.

A comparison of the proposed PI current controller with PSO and ZN controllers response at $R_a = 50\%$, 75%, 100%, and 150% of its rated value are given in Fig. 9. Fig. 9 clearly illustrates the outperformance of the proposed PI current controller over both PSO and ZN controllers. This indicated that the motor can run with the proposed PI in safe and secure fashion than the other two PI technique during transient operations. To evaluate the effectiveness of the proposed PID speed controller, its performance is tested at different armature resistance values and different moment of inertia J values and then compared with PSO and ZN PID controllers. In Fig. 10, the PID speed controller is tested at three armature resistance R_a values; 50%, 100%, 150% of its rated value. Fig. 9 shows that the PID controller response is not affected by varying the armature resistance. In Fig. 11, the PID speed controller is tested at three moment of inertia J values; 50%, 100%, 150% of its rated value.

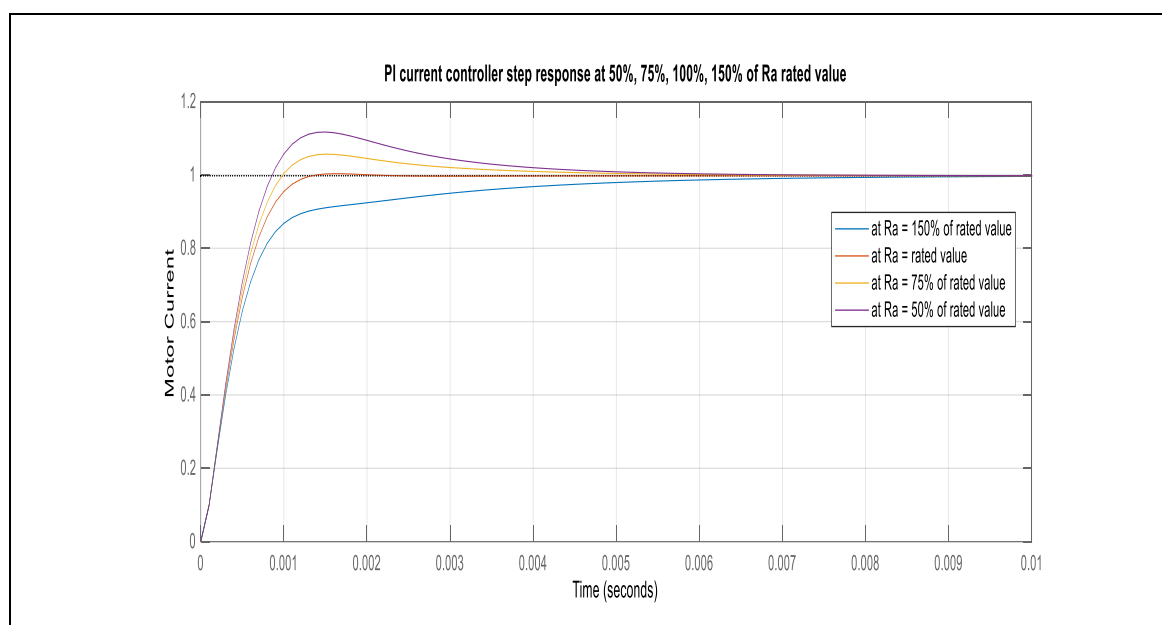
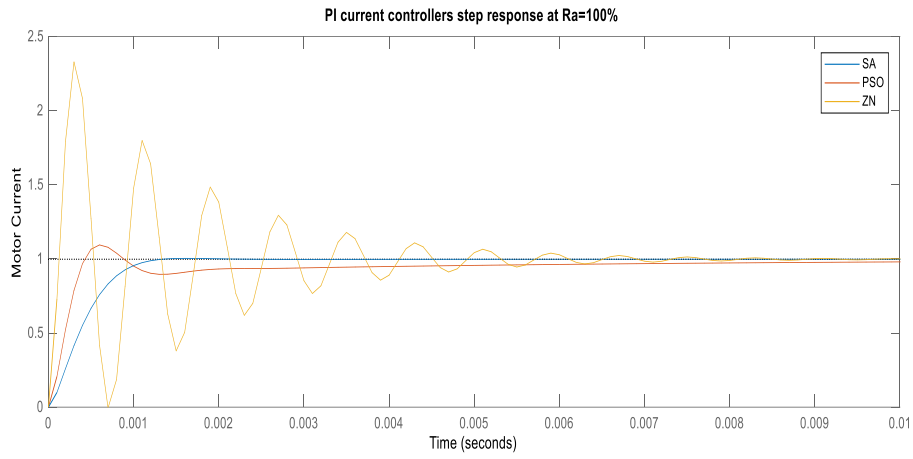
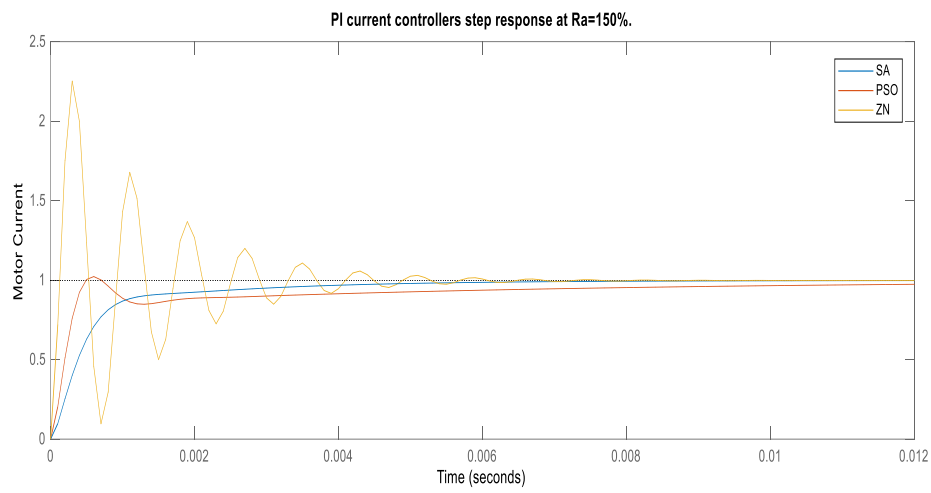


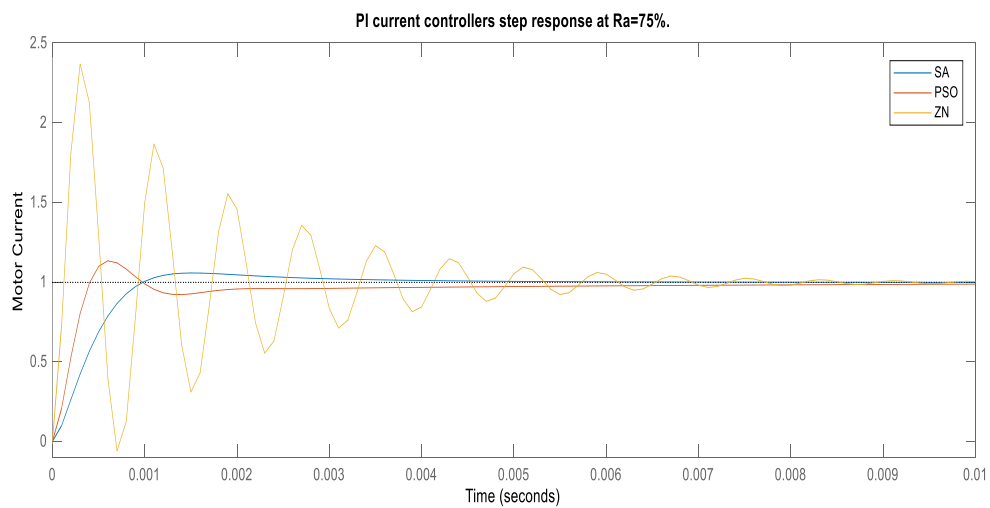
Fig. 8 PI current controller step response at $R_a = 50\%$, 75%, 100%, and 150% of its rated value.



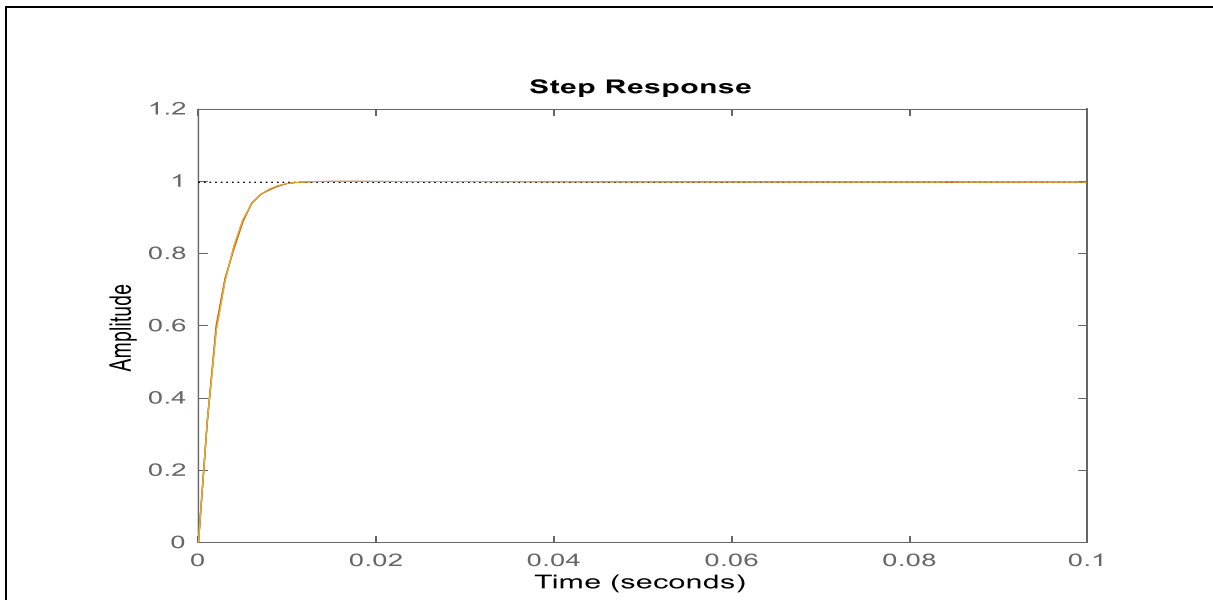
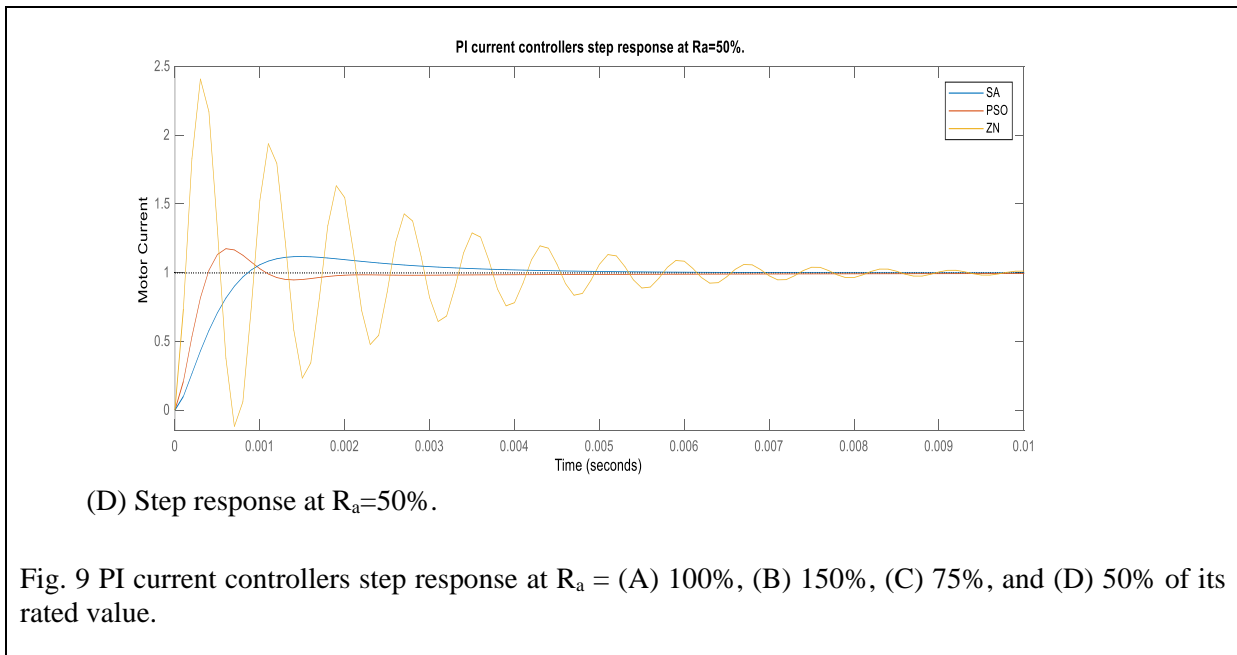
(A) Step response at $R_a=100\%$.



(B) Step response at $R_a=150\%$.



(C) Step response at $R_a=75\%$.



We compare our SA PID controller, with both PSO and ZN controllers. The transfer function of PID speed controller designed by Ziegler-Nichols is given by [20]

$$G_{PID_PSO}(s) = 4.623 \frac{(0.013827 s^2 + 0.0569 s + 1)}{0.0569 s} \quad (15)$$

$$G_{PID_ZN}(s) = 208.8 \frac{(5.0625 \times 10^{-8} s^2 + 4.5 \times 10^{-4} s + 1)}{4.5 \times 10^{-4} s} \quad (14)$$

where $K_p = 208.8$, $T_i = 4.5 \times 10^{-4}$, $K_i = 464000$, $T_d = 1.125 \times 10^{-4}$, $K_d = 0.02349$.

Fig. 12 illustrates the step responses of three PID speed controllers at the rated values of R_a and J . This clearly shows the superiority the proposed SI PID controller over the other two PID controllers in running the motor with a speed response having 0% overshoot and minimal rise time and settling time.

The transfer function of the PSO PID speed controller designed by Bayoumi and Soliman [20] is given by

The three PID controllers are compared at 50% and 150% of the rated armature resistance. Fig. 13 illustrate the step responses of the three controllers at 50% of R_a

while Fig. 14 illustrate the step responses of the three controllers at 150% of R_a .

The three PID controllers are then evaluated at 50% and 150% of the rated moment of inertia J . Fig. 15 illustrate the step responses of the three controllers at 50% of J while Fig. 16 illustrate the step responses of the three controllers at 150% of J .

3 Conclusion

This work proposes a simple yet effective approach for PI current controller and PID speed controller for a

PMBLDC motor drive system. The controller's parameters are optimized to simultaneously minimize three response parameters indices; maximum-overshoot, rise time and settling time for each controller. The tuning process is performed using the Simulated Annealing optimization technique. The proposed approach was tested over PMBLDC motor parameters variations and the results show that the proposed approach outperforms Particle Swarm Optimization and Ziegler-Nichols tuning methods.

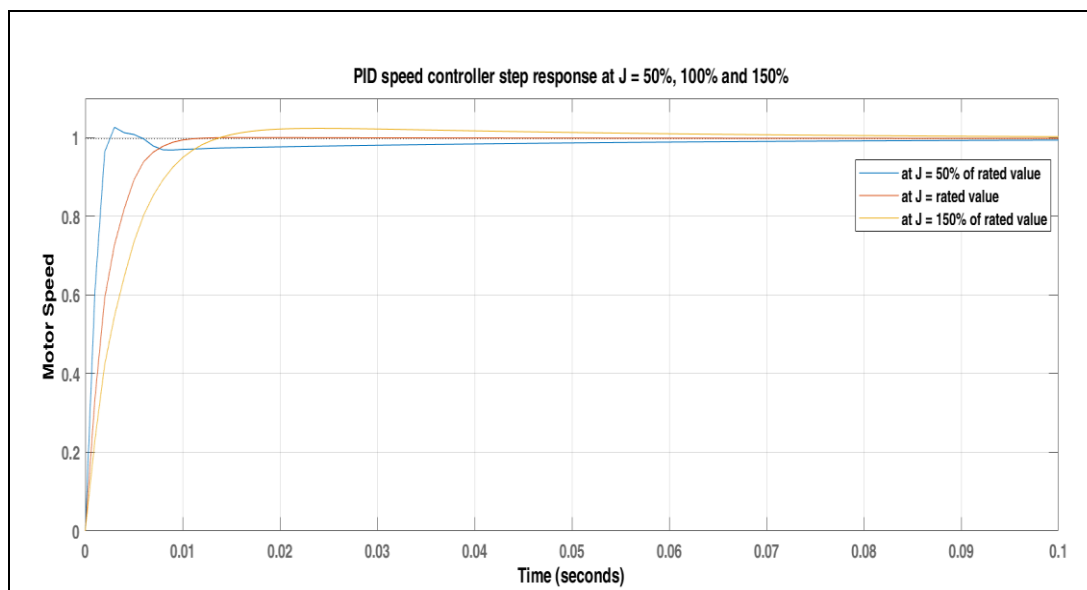
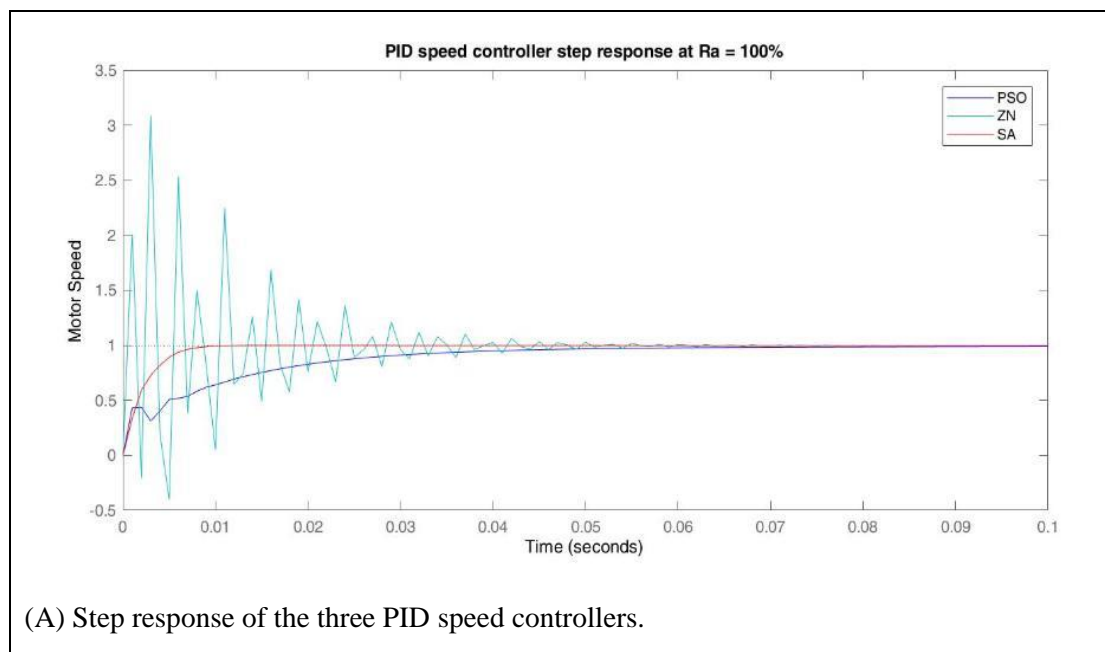
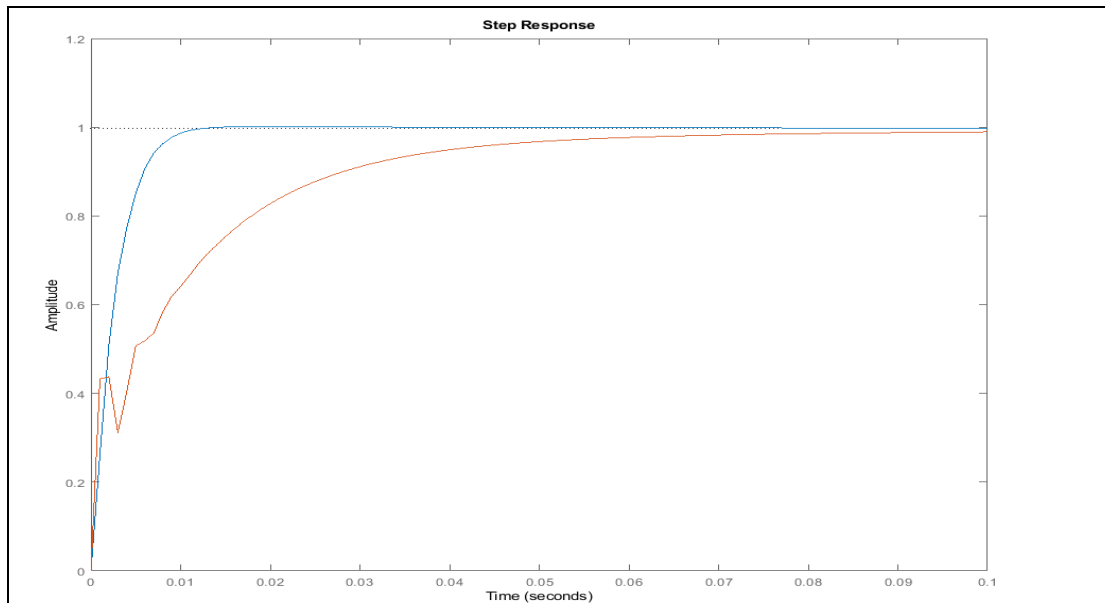


Fig. 11 Proposed PID speed controller step response at $J = 50\%$, 100% , 150% of its rated value.

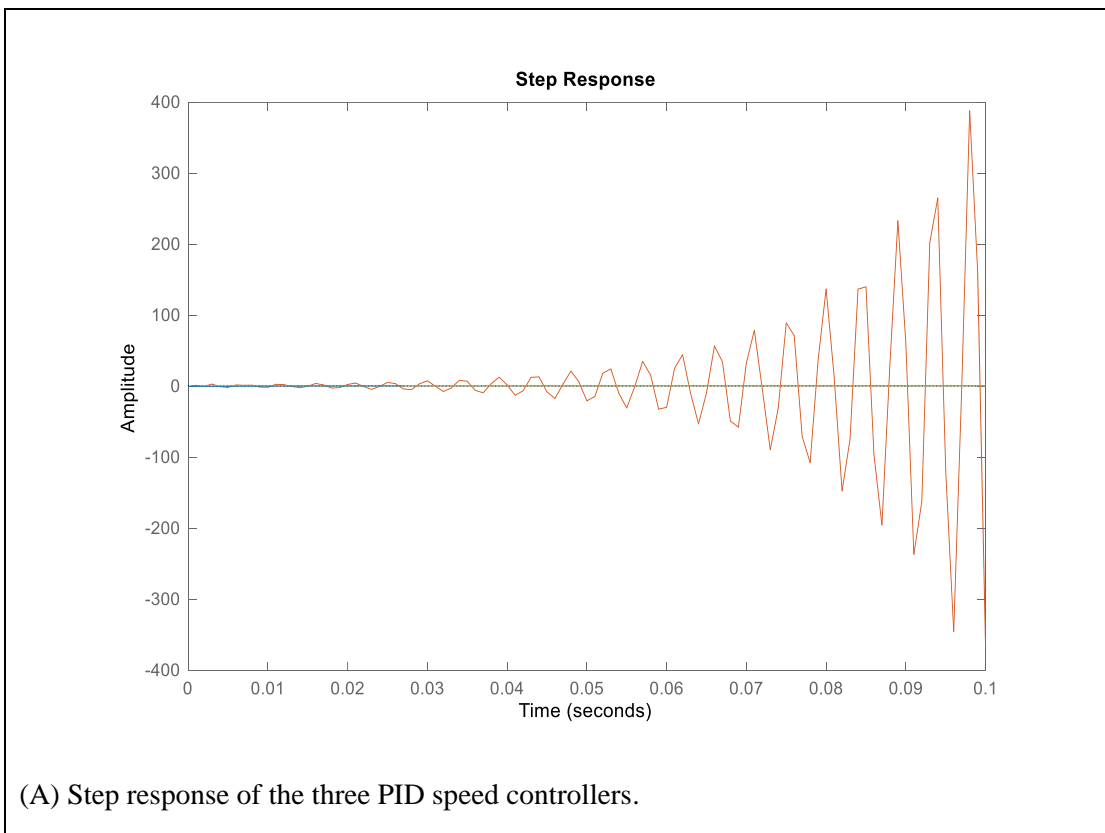


(A) Step response of the three PID speed controllers.



(B) Step response of SI and PSO speed controllers.

Fig. 12 PID speed controllers step response at $R_a=100\%$ and $J =100\%$.



(A) Step response of the three PID speed controllers.

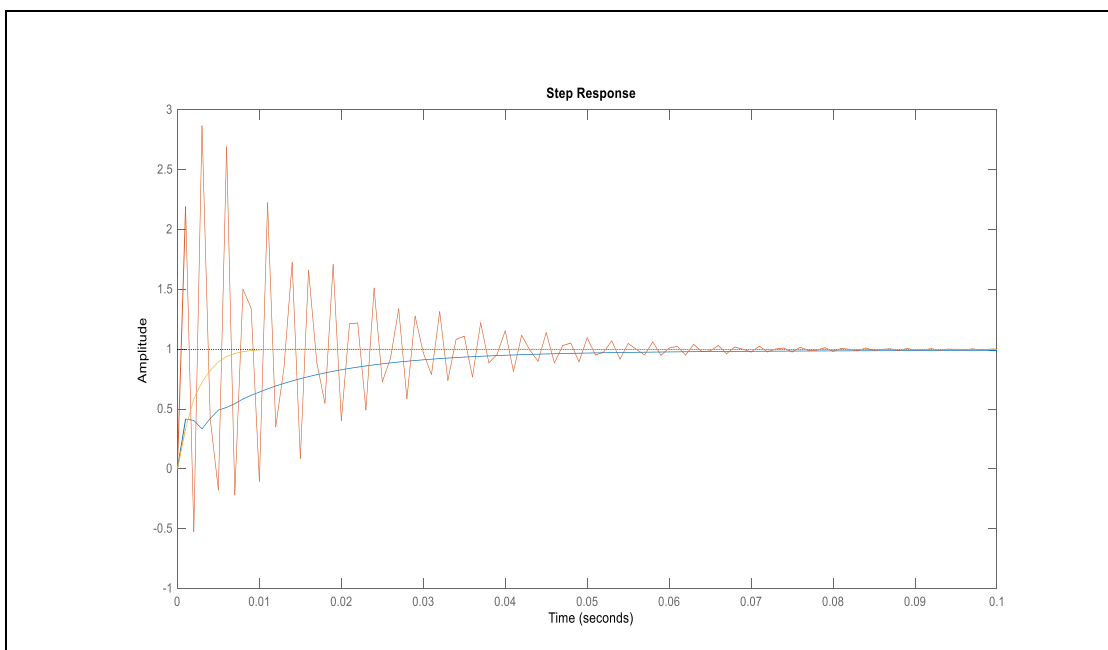
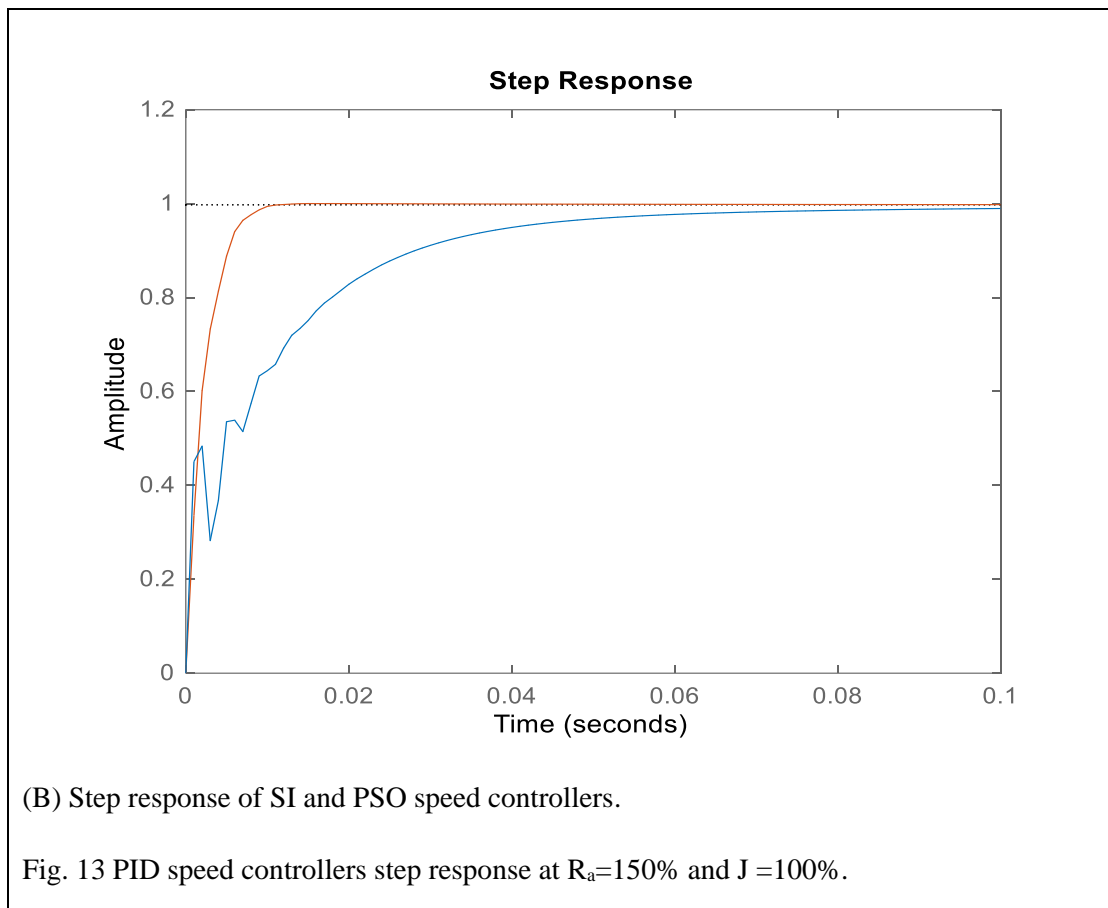
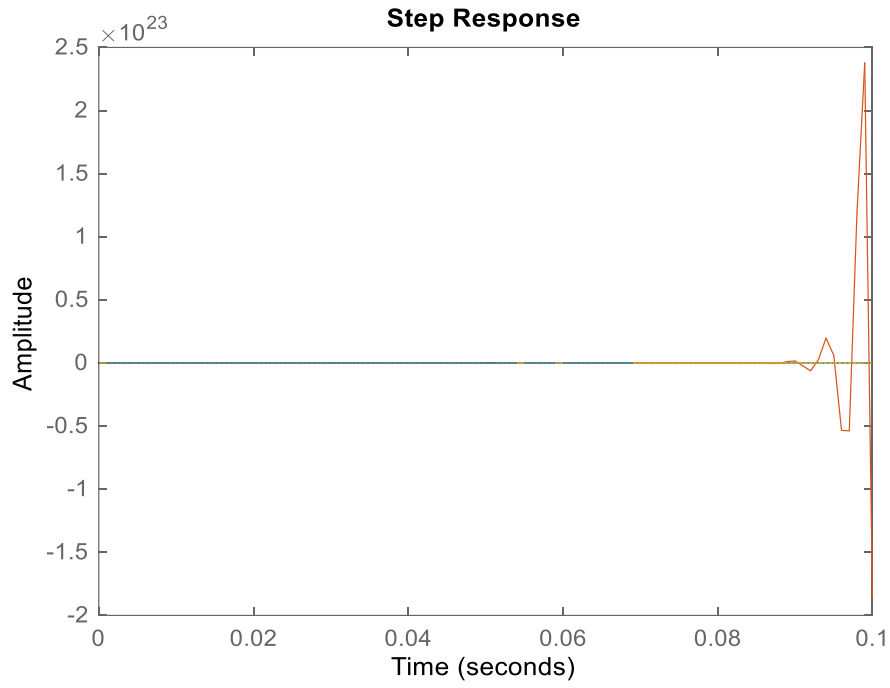
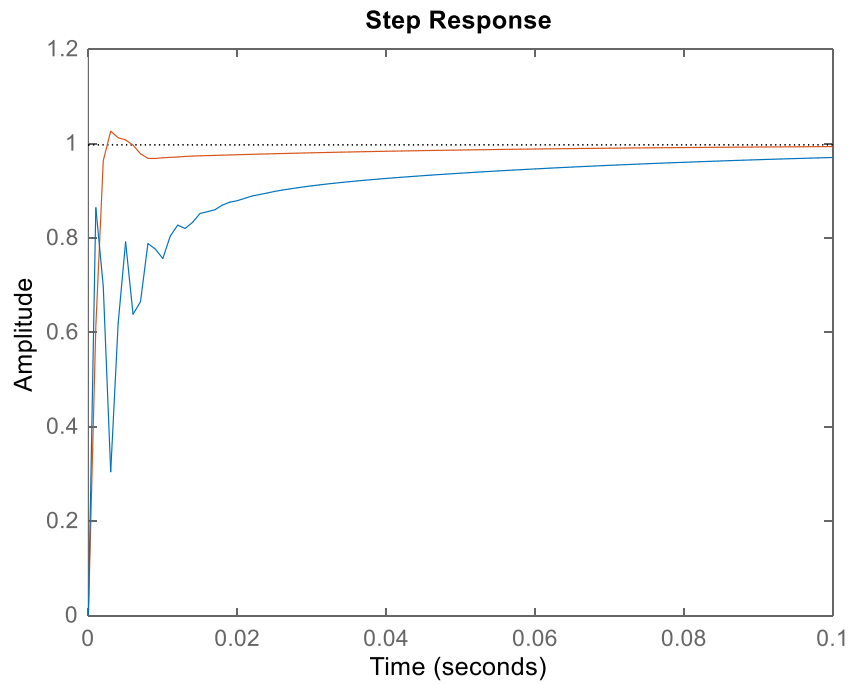


Fig. 14 Step response of the three PID speed controllers step response at $R_a=150\%$ and $J=100\%$.

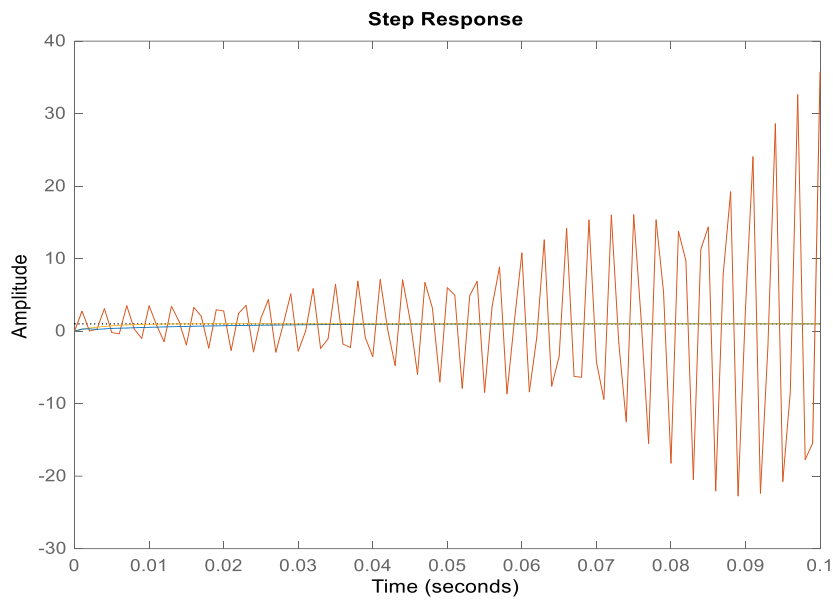


(A) Step response of the three PID speed controllers.

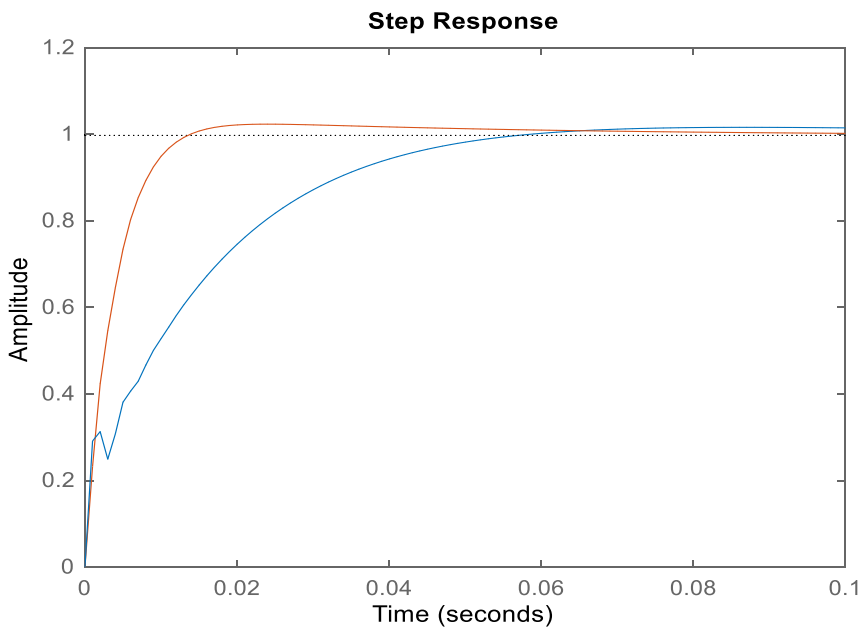


(B) Step response of SI and PSO speed controllers.

Fig. 15 PID speed controllers step response at $R_a=100\%$ and $J=50\%$.



(A) Step response of the three PID speed controllers.



(B) Step response of SI and PSO speed controllers.

Fig. 16 PID speed controllers step response at $R_a=100\%$ and $J =150\%$.

Appendix

Table 1: The PMBLDCM drive parameters.

Power	373 W
Current	17.35 A
Voltage	160 V
Torque	0.89 N.m
Phase resistance (R_a)	1.4 Ω
Phase inductance (L_a)	2.44 mH
Moment of inertia (J)	0.0002 kg m ²
Motor friction (B)	0.002125 N.m/rad/sec
EMF constant (K_b)	0.0513 Vs

Table 2: The converter and transducers parameters.

Converter gain (K_r)	16 V/V
Converter time constant (T_r)	50 μ s
Current transducer gain (K_c)	0.288 V/A
Current transducer time constant (T_c)	0.159 ms
Speed transducer gain (K_w)	0.0239 Vs
Speed transducer time constant (T_w)	1ms

References:

- [1] C. C. Chan and K. T. Chau, "An Overview of Power Electronics in Electric Vehicles", IEEE Trans. on Ind. Electron., vol. 44, no.1, pp. 3-13, Feb. 1997.
- [2] L. Ben-Brahim y A. Kawamura, "A Fully Digitized Field-Oriented Controlled Induction Motor Drive Using Only Current Sensors", IEEE Trans. on Ind. Electron., vol. 39, no. 3, pp. 241-249, June 1992.
- [3] Y. Xue, X. Xu, T. G. Habetler y D. M. Divan, "A Stator Flux-Oriented Voltage Source Variable-Speed Based on DC Link Measurement," IEEE Trans. on Ind. Applicat., vol. 27, no.5, pp. 962-069, Sept/Oct. 1991.
- [4] E.H.E. Bayoumi, "An improved approach of position and speed sensorless control for permanent magnet synchronous motor," Electromotion Scientific Journal, vol.14, pp. 81-90, 2007.
- [5] A. R. Millner, "Multi-Hundred Horsepower Permanent Magnet Brushless Disc Motors," in Proc. IEEE APEC Applied Power Electronics Conference, 1994, pp. 351-355.
- [6] P. Pillay, R. Krishnan, "Application Characteristics of Permanent Magnet Synchronous and Brushless DC Motors for Servo Drives," IEEE Trans. on Ind. Applicat., vol. 27, no.5, pp. 986-996, Sept/Oct. 1991.
- [7] T. Low and M.A. Jabbar, "Permanent-Magnet Motors for Brushless Operation," IEEE Trans. on Ind. Applicat., vol. 26, no.1, pp. 124-129, Jan/Feb 1990.
- [8] P.C. Krause, "Analysis of Electric Machinery," McGraw-Hill Company, 1987, pp.499-534.
- [9] P. Yedamale, "Brushless DC (BLDC) Motor Fundamentals," Microship Technology Inc., 2003, pp.1-20.
- [10] Ziegler, J. G., Nichols, N. B., "Optimum settings for automatic controllers," Trans. ASME, vol. 62, pp. 759-768, 1942.
- [11] Astrom, K. J. and Hagglund, T., "PID controller," 2nd Edition, Instrument of Society of America, Research triangle park, North Carolina, 1995.
- [12] Morari, M., and Zafiriou, E., "Robust process control," Prentice Hall, USA, 1989.
- [13] Rivera, D. E., Morari, M., and Skogestad, S., "Internal model control - PID control design", Ind. Eng. Chem. Process Des. Dev., 25, pp. 252-265, 1986.
- [14] Cohen, G. H. and Coon, G. A., "Theoretical considerations of retarded control," Trans. of ASME, vol. 75, pp. 827, 1953.
- [15] Feng, Z., Wang, Q. G. and Lee, T. H., "On the design of multivariable PID controllers via LMI approach," Automatica, vol. 38, pp. 517-526, 2002.
- [16] Ge, M., Chiu, M. and Wang, Q. G., "Robust PID controller design via LMI approach," J.Process Control, vol.12, pp. 3-13, 2002.
- [17] Ali W.H, Zhang Y, Akujuobi C.M, Tolliver C.L and Shieh L.S, "DSP-Based PID controller design for the PMDC motor," I.J. Modeling and Simulation, Vol 26, No 2, pp143-150, 2006.
- [18] Changliang Xia, PeiJian Guo, Tingna Shi, Minghao Wang, "Speed control of brushless DC motor using genetic algorithm based fuzzy controller", 2004 International Conference on Intelligent Mechatronics and Automation, Chengdu, China, 26-31 Aug. 2004.
- [19] Picardi C., Rogano N., "Parameter Identification of Induction Motor Based on Particle Swarm Optimization," International Symposium on Power Electronics, Electric Drives, Automation and Motion, May 23-26, 2006.

- [20] Ehab H.E. Bayoumi, Hisham M. Soliman, "PID/PI tuning for minimal overshoot of permanent-magnet brushless DC motor drive using particle swarm optimization", *Electromotion Scientific Journal*, Vol. 14, No. 4, pp.: 198-208, 2007.
- [21] Kennedy, J. and Eberhart, R.C. *Swarm Intelligence*, Morgan Kaufmann, San Francisco, 2001.
- [22] Ehab H.E. Bayoumi, "Parameter estimation of cage induction motors using cooperative bacteria foraging optimization", *Electromotion Scientific Journal* Vol. 17, No. 4, pp: 247-260, 2010.
- [23] El-Abd, M. and Kamel, M., "A taxonomy of cooperative search algorithms," *Proceedings of the 2nd International Workshop on Hybrid Metaheuristics*, pp.32-41, 2005.
- [24] R.Krishnan, "Permanent Magnet Synchronous and Brushless DC Motor Drives: Theory, Operation, Performance, Modelling, Simulation, Analysis and Design, Part 3: Permanent Magnet Brushless DC Machines and Their Control," Virginia Tech, Blacksburg, 2000.
- [25] Bhaskara, R. M., de Brevern, A. G., Srinivasan, N., 2012. Understanding the role of domain-domain linkers in the spatial orientation of domains in multi-domain proteins. *Journal of Biomolecular Structure and Dynamics*, 1-14.
- [26] Vega-Rodriguez, M. A., Gomez-Pulido, J. A., Alba, E., Vega-Perez, D., Priem-Mendes, S., Molina, G., 2007. Evaluation of different metaheuristics solving the rnd problem. In: *Applications of Evolutionary Computing*. Springer, pp. 101-110.
- [27] Mendes, S. P., Molina, G., Vega-Rodriguez, M. A., Gomez-Pulido, J. A., Saez, Y., Miranda, G., Segura, C., Alba, E., Isasi, P., Leon, C., et al., 2009. Bench- marking a wide spectrum of metaheuristic techniques for the radio network design problem. *Evolutionary Computation, IEEE Transactions on* 13 (5), 1133-1150.
- [28] Busetti, F., 2003. Simulated annealing overview.
- [29] Henderson, D., Jacobson, S. H., Johnson, A. W., 2003. The theory and practice of simulated annealing. In: *Handbook of metaheuristics*. Springer, pp. 287-319.
- [30] Geman, S., Geman, D., 1984. Stochastic relaxation, gibbs distributions, and the bayesian restoration of images. *Pattern Analysis and Machine Intelligence, IEEE Transactions on* (6), 721-741.
- [31] Salamon, P., Sibani, P., Frost, R., 2002. Facts, conjectures, and improvements for simulated annealing. *SIAM*.
- [32] Ingber, L., 1993. Simulated annealing: Practice versus theory. *Mathematical and computer modelling* 18 (11), 29-57.
- [33] Smith, K. I., Everson, R. M., Fieldsend, J. E., Murphy, C., Misra, R., 2008. Dominance-based multiobjective simulated annealing. *Evolutionary Computation, IEEE Transactions on* 12 (3), 323-342.
- [34] Jaraiz-Simon, M. D., Gomez-Pulido, J. A., Vega-Rodriguez, M. A., Sanchez- Perez, J. M., 2013. Simulated annealing for real-time vertical-handoff in wireless networks. In: *Advances in Computational Intelligence*. Springer, pp. 198-209.
- [35] Kundu, S., Mahato, M., Mahanty, B., Acharyya, S., 2008. Comparative performance of simulated annealing and genetic algorithm in solving nurse scheduling problem. In: *Proceedings of the International MultiConference of Engineers and Computer Scientists*. Vol. 1.
- [36] Bertsimas, D., Nohadani, O., 2010. Robust optimization with simulated annealing. *Journal of Global Optimization* 48 (2), 323-334.
- [37] Huang, K.-Y., Hsieh, Y.-H., 2011. Very fast simulated annealing for pattern detection and seismic applications. In: *Geoscience and Remote Sensing Symposium (IGARSS), 2011 IEEE International*. IEEE, pp. 499-502.
- [38] Tomshine, J., Kaznessis, Y. N., 2006. Optimization of a stochastically simulated gene network model via simulated annealing. *Biophysical journal* 91 (9), 3196-3205.
- [39] Ishikawa, M., Toya, T., Hoshida, M., Nitta, K., Ogiwara, A., Kanehisa, M., 1993. Multiple sequence alignment by parallel simulated annealing. *Computer applications in the biosciences: CABIOS* 9 (3), 267-273.
- [40] Kim, J., Pramanik, S., Chung, M. J., 1994. Multiple sequence alignment using simulated annealing. *Computer applications in the biosciences: CABIOS* 10 (4), 419-426.
- [41] Kirkpatrick, S., Jr., D. G., Vecchi, M. P., 1983. Optimization by simulated annealing. *Science* 220 (4598), 671-680.